ELSEVIER

Optics and Lasers in Engineering 38 (2002) 333–359

OPTICS and LASERS in ENGINEERING

An eye behavior measuring device for VR system

Chern-Sheng Lin*

Department of Automatic Control Engineering, Feng Chia University, Taichung, Taiwan, ROC

Received 1 October 2001; received in revised form 1 December 2001; accepted 1 February 2002

Abstract

This work presents an eye-tracking and pupil size-measuring device that interfaces with a computer for applications useful in psychometry, ophthalmology, physiology and virtual reality (VR) systems. This system utilizes a change-coupled device (CCD) camera, appropriate lenses, PC with frame grabber and a DSP unit with various types of VR equipment, i.e., HMD, simulator or LCD projection device. The digital signal processing unit is used to calculate the average brightness and contrast of the VR video image. A CCD camera with various attachments can be mounted on various VR systems to capture the human eye image for testing. An image capture card and a personal computer are used to analyze the test image. From the eye digital image, the computer obtains data on the pupil size and a trace of the tested eye. A pattern recognition computer program and five measurement parameters are used to distinguish the position of the pupil, calculate the pupil location coordinate and analyze the physical conditions of the user. These data can be plotted against the average brightness and contrast of the VR video image in real time. This information is shown on the screen of a personal computer and used for cross-link analysis. This eye-tracking interface can determine the position of a subject's pupil and map that position into a display point on a computer screen. The pupil size and location data versus the average brightness and contrast of a VR video image are computed in real time.

Keywords: Eye-tracking device; Pattern recognition; The position of the pupil

1. Introduction

With the progress in technology over the past several years, "virtual reality" (VR) has been applied in several fields, such as art, medical diagnosis, entertainment,

*Tel.: +886-4-451-7250; fax: +886-4-451-9951.
E-mail address: cslin@auto.fcu.edu.tw (C.-S. Lin).

0143-8166/02/$ - see front matter
PII: S0143-8166(02)00034-9

communications, computer science, and so on. Today's VR equipment is varied in functionality and purpose. The present VR equipment can address several human sensorial channels [1]. Many new VR applications are expected in the coming years and many hardware and software configurations will become possible owing to improvements in technological development. More and more people are concerned with the subject's responses when engaged with a VR system. How excited is the user? What is the most interesting point that the user sees on the VR screen? No one can answer these questions. This reflects the fact that this is a new research field. It is therefore natural that we would design an eye-behavior-measuring device for VR systems incorporated with an eye-tracking mechanism.

To observe eye movement, several eye-tracking systems have been developed [2–6], such as the "piezoelectric eye-tracking system", the "magnetic eye-tracking system", and the "image eye-tracking system". The object of these systems is to detect eye movement in real time. For example, the piezoelectric eye-tracking system detects eye movement based on the electrical measurement of the difference in potential between the cornea and the retina. Essentially, eye movements are accompanied by the appearance of electric signals. In front of the head, the corneal to retinal potential creates an electric field, which changes in orientation as the eyeballs rotate. Electrodes made of piezoelectric material placed near the eyes can detect these electrical signals. However, sweat may affect the electrical signal read out.

The magnetic eye-tracking operational system is similar to that of the piezoelectric eye-tracking system. A magnetic field is created around the eyeball, in which the eye movement can be observed after signal processing. Another eye-movement-tracking system is the image eye-tracking system. One method of applying this tracking system is one-point [7] or linear scanning, which is a rapid scanning process. However, when the eye moves quickly, the eye images shown in a monitor cannot be precisely distinguished from one another. Another method of applying this tracking system is matrix scanning. According to this method, the eye orientation when viewing a two-dimensional object and the size of the pupil can be measured and recorded. This system is an important tool for psychologists because the data produced by the pupil-tracking system are useful in psychometry research. In this method, the eye orientation indicates the area in the two-dimensional object that the user is viewing. The eye (pupil) orientation can be recorded and displayed on a video screen. The "image type eye-tracking system" is more adaptable than the piezoelectric eye-tracking system. However, the conventional image eye-tracking system cannot be combined with various VR systems. This eye-tracking method requires the user's head to remain totally motionless, otherwise point of regard information is lost; also, the eye will become out of focus [8] if very large eye movements are involved.

Here, we designed a new adaptive eye-tracking system (Fig. 1) [9,10] for measuring all the information of eye movements, pupil size, screen brightness and contrast. This system can be coupled with a change-coupled device (CCD), appropriate lenses, PC with frame grabber and a DSP unit with various types of VR equipment, such as head mounted display (HMD), simulator or LCD projection. A VR display device, for example a video screen, computer monitor, head mounted display device or

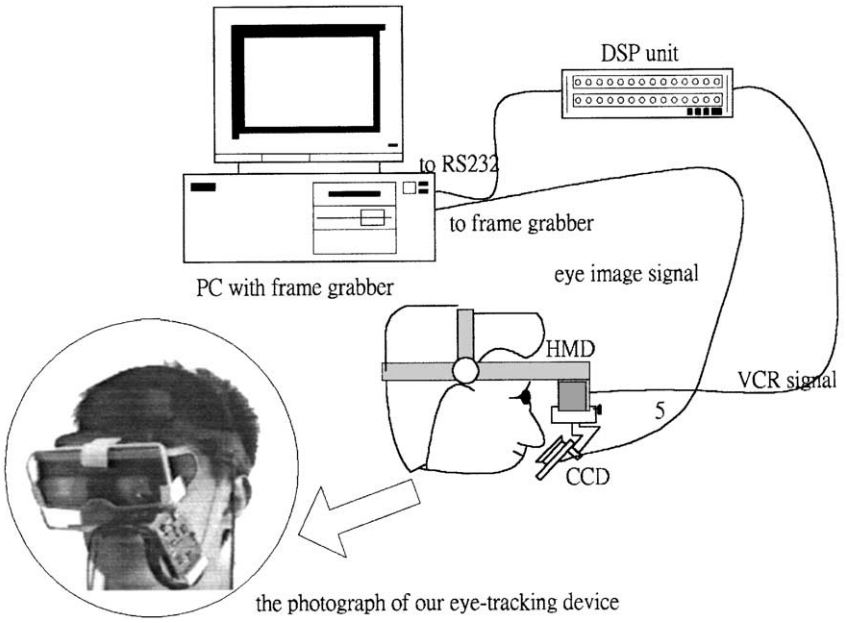

Fig. 1. The arrangement of the eye measurement system for immersion VR.

projection screen, can provide a video image for an observer. The CCD camera used in this system was built from an observation camera component set. On the back of this camera, a mini sender was mounted, to transmit the video signal to a frame grabber at the computer. The user must set the camera just in front and under the subject's face and focus the camera onto one of the subject's eyes. This system can judge the gazing direction and eye conditions from information on the gray level, pixel locations, and histogram of the eye image (Fig. 2) using special image processing algorithms [11–16] and five evaluation parameters. The video signals from

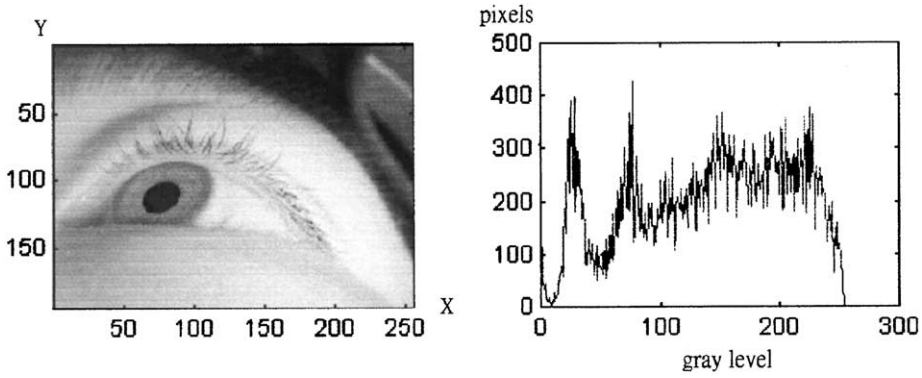

Fig. 2. The histogram of an eye image.

the VR display device are tested and evaluated using a digital signal processing (DSP) unit. The resulting signals, including the contrast and brightness data from the VR display device, are transmitted from the DSP unit to the PC. The PC subsequently processes and analyzes the image data from the image capture card and the resulting signals from the DSP unit. With this information, the PC then produces data on the pupil gaze location, pupil area, and brightness and contrast of the video screen.

We will discuss the construction of this system, the image-processing approach and the eye measuring function. The computer will process the eye image captured by the CCD automatically and determine the subject's eye activity. This system is able to digitally record where someone is looking. Having this information available in real time allows the use of these systems in psychometric analysis. The eye-tracking equipment produced by many companies is expensive and uncomfortable, requiring the user's head to be fixed into a frame. Most researchers feel that this equipment is useful only for laboratory experiments. In our HMD eye-tracking system, the on-line eye-track-processing device is transportable and comfortable for the user in a multitude of applications. This equipment is not expensive and has the potential to be reduced in size and weight.

2. Image processing for eye behavior evaluation

This measurement system provides a method for tracking eye movements and measuring the pupil area for applications in psychometry, ophthalmology, physiology research and VR systems. Image processing with this system is comprised of the following steps:

1. Capturing the subject's eyeball image using a detachable image-capturing device.
2. Calculating the eyeball position and pupil area from the captured eyeball image, utilizing image processing.
3. Displaying the test image on the VR screen and transmits it to a DSP unit coupled to the VR display device in real time.
4. Calculating an average brightness value or contrast value for the test image using a computer.
5. Analyzing the average brightness or contrast value, the eyeball position and pupil area.
6. Recording and reporting the data for all the calculated items.

The eye behavior evaluation is complicated by its dependence upon both individual and general parameters. The individual parameters are the user's visual activity, resolution, and detection characteristics. For example, the diameter of a pupil changes fully from 2 to 7 mm during emmetropia. In our system, this range of values is usually from 3 to 5 mm under the same luminance conditions. Too many parameters affect the pupil size and the inter-subject variability is high. Different people have different-sized pupils. The diameter of the pupil is also affected by

various general parameters, such as the lighting level of the viewed scene, luminance contrast between the region of interest and its background, the time allowed for the observation and the type of scenario viewed. The relative alterations in the diameter of the pupil must be calculated to evaluate the eye behavior. The speed of the target's motion, the number of colors in the scene, the brightness of the colors in the region of interest and the subject's static or dynamic visual acuity are other general parameters. The eye-tracking results depend upon many of these parameters. The first goal of this eye-tracking technology is therefore eye feature extraction using an image processing method. Amini et al. [17] had developed a parallel algorithm for determining two-dimensional object positions. The boundaries of pupils also provide important features in recognition of the eye's location of visual image. Here vertical and horizontal lines are used to check the eye location (Fig. 3). The area of every line is 20 pixels. In a 640×480 image, we can obtain 32×24 boxes in this image. Let A_i, B_i, C_i, … represent the intersections of the lines in Fig. 3. A 4×4-sized box was selected as the search box. The procedures for this algorithm are:

1. Check the pixels of the image using the search box from left to right and up and down. Check only the right and bottom side of the box, for example, the horizontal line segment $B_0\ B_1$, and the vertical line segment $A_1\ B_1$.
2. Let X_i or Y_i represent the vertical or horizontal line segment of the box. Summarize the dark pixels in the vertical or horizontal line segments of the ith box, i.e., $\mathrm{Sum}(X_i)$ or $\mathrm{Sum}(Y_i)$:

$$\mathrm{Sum}(X_i) = \sum \Theta\{p(x, y)\}, \quad p(x, y) \in X_i,$$

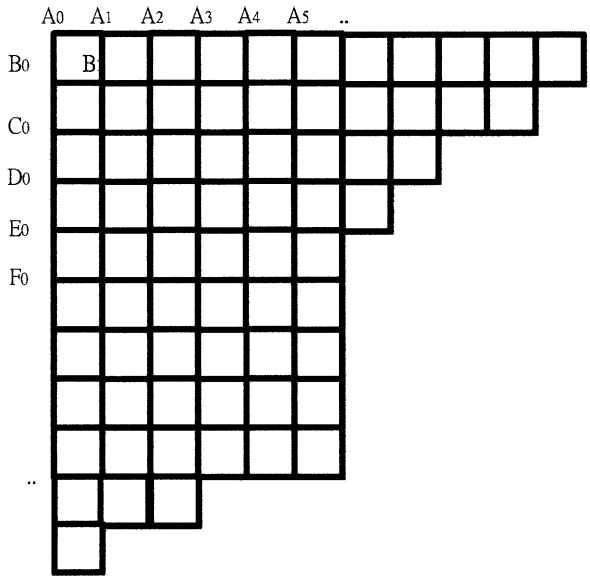

Fig. 3. The search path in the pupil analysis.

where

$$\Theta\{p(x,\ y)\} = \begin{cases} 0 & \text{when pix}\,(x,y) \geqslant T, \\ 1 & \text{when pix}\,(x,y) < T \end{cases}$$

with pix(x, y) being the gray level of the pixel $p(x, y)$ and T is the threshold value. We can establish another threshold value E_1. The values of T and E_1 depend on the light field of the hardware and are adjustable. If Sum(X_i) and Sum(Y_i) are smaller than the thresholds for $4 \times E_1$, then check the next box.

3. Otherwise, when the values for Sum(X_i) or Sum(Y_i) are greater than $4 \times E_1$ an expanding box is adopted to envelop the dark object. In an expanding box

$$\begin{aligned} &\text{the top margin } Y_i: \ \ \text{Sum}\,(Y_{i+1}) \geqslant n \times E_1 \text{ and Sum}(Y_i) < n \times E_1, \\ &\text{the bottom margin } Y_j: \ \ \text{Sum}(Y_{j-1}) \geqslant n \times E_1 \text{ and Sum}(Y_j) < n \times E_1, \\ &\text{the left margin } X_i: \ \ \text{Sum}(X_{i+1}) \geqslant n \times E_1 \text{ and Sum}(X_i) < n \times E_1, \\ &\text{the right margin } X_j: \ \ \text{Sum}(X_{i-1}) \geqslant n \times E_1 \text{ and Sum}(X_i) < n \times E_1, \end{aligned}$$

where n is the number of spaces. As shown in Fig. 4(A), the gray level summation of line Sum(Y_4) is lower than that for $4 \times E_1$. The upper margin of the expanding box will be set at line Y_3. The left margin line X_0 to X_{-1}, and right margin X_4 will be extended to X_4 and the bottom margin Y_8 is obtained. Fig. 4(B) shows another example. Sum(Y_4) and Sum(X_4) have lower values than $4 \times E_1$. The upper and left margins of the expanding box are set to Y_1 and X_{-1}. The bottom and right margins of the expanding box are set to Y_7 and X_7. The size of the expanding box may be 4×4, 4×5, 5×5, or 6×6, or some other value. This means that the expanding box will grow larger and larger until the dark object is totally inside the box.

4. After determining the approximate pupil locations in the expanding box, the circular factor s of the object is calculated to verify that the dark part of the image is the pupil.

$$s = \frac{l^2}{A},$$

where l is the length of the edge of a dark object and A is its area.

If the circular factor s is smaller than the threshold E_2, the dark object is the pupil.

This pattern recognition computer method is useful for distinguishing the position of the eye and calculating the coordinates of the center of the pupil (Fig. 5) to create an "eye window". Thereafter, the pixels representing the area of the pupil are converted into the actual value for the pupil area. After calculating the values for the pupil area from a plurality of images, pupil-area evaluation over a period of time can be obtained. The measurement system provides an apparatus for tracking eye movement and measuring the pupil area for applications in a VR or an other system in which the image-capturing device must be detachable. The eye tracking and pupil measurement areas are provided to obtain eye movement, pupil dilation and

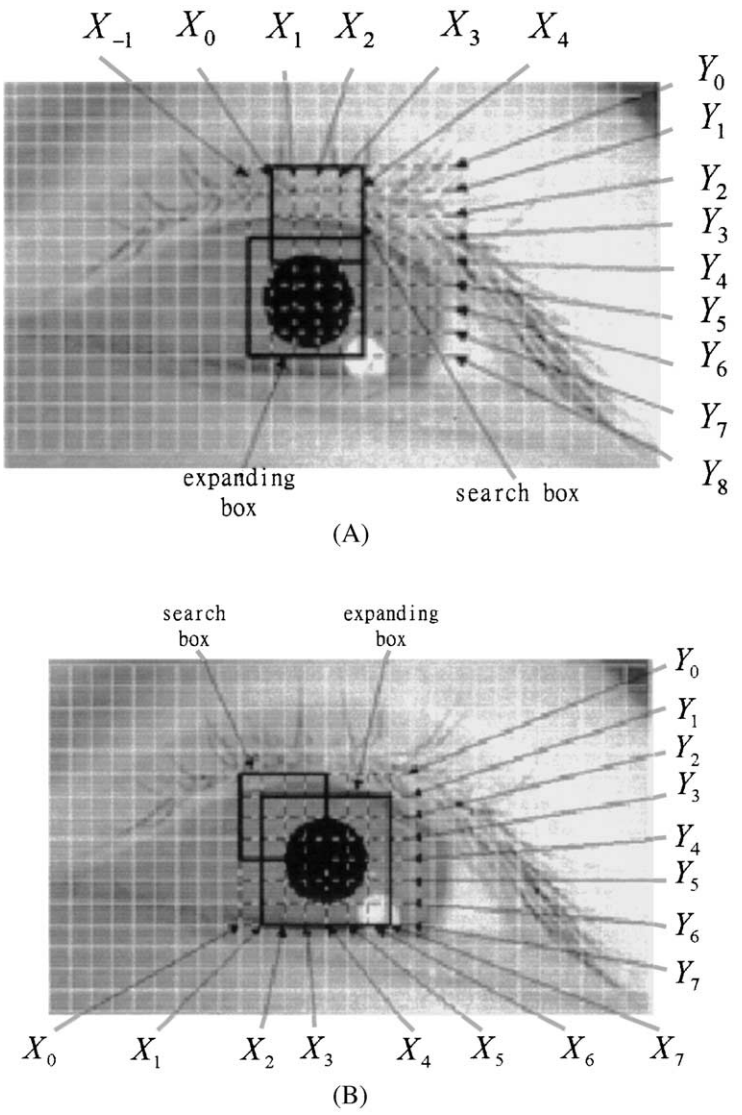

Fig. 4. The search and expansion boxes for measuring pupil contractions and dilations.

contraction data. This system calculates the brightness and contrast of the VR video signal and displays the data on a computer screen (Fig. 6).

The resulting location of the eyeball and the area of the pupil are then evaluated and transmitted to a buffer of PC in real time. Meanwhile, a calculated pupil area value, A_p, an average brightness value, X_{av}, and a contrast value, C, processed by the DSP unit, are displayed on a monitor in real time. Additionally, the graphs illustrating the calculated pupil area value, A_p, the average brightness value, X_{av}, and the contrast value, C, versus time are displayed in the frame in real time.

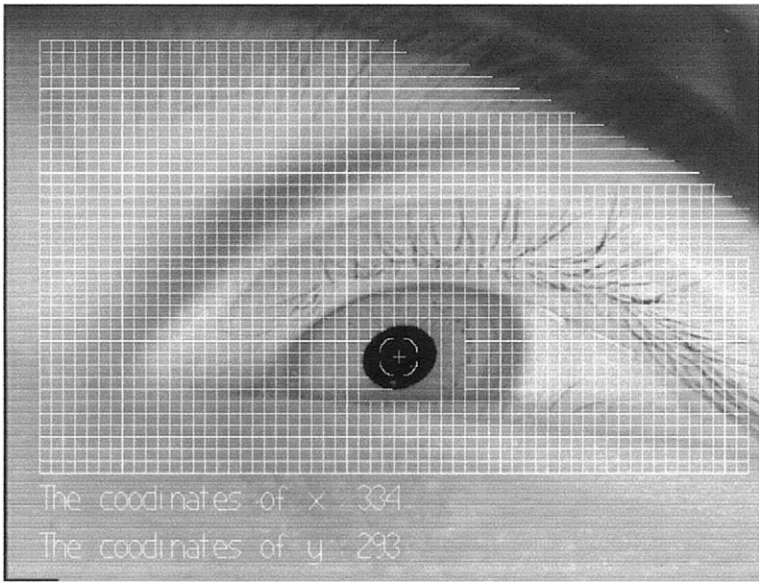

Fig. 5. A pattern recognition computer program used to distinguish the position of the pupil.

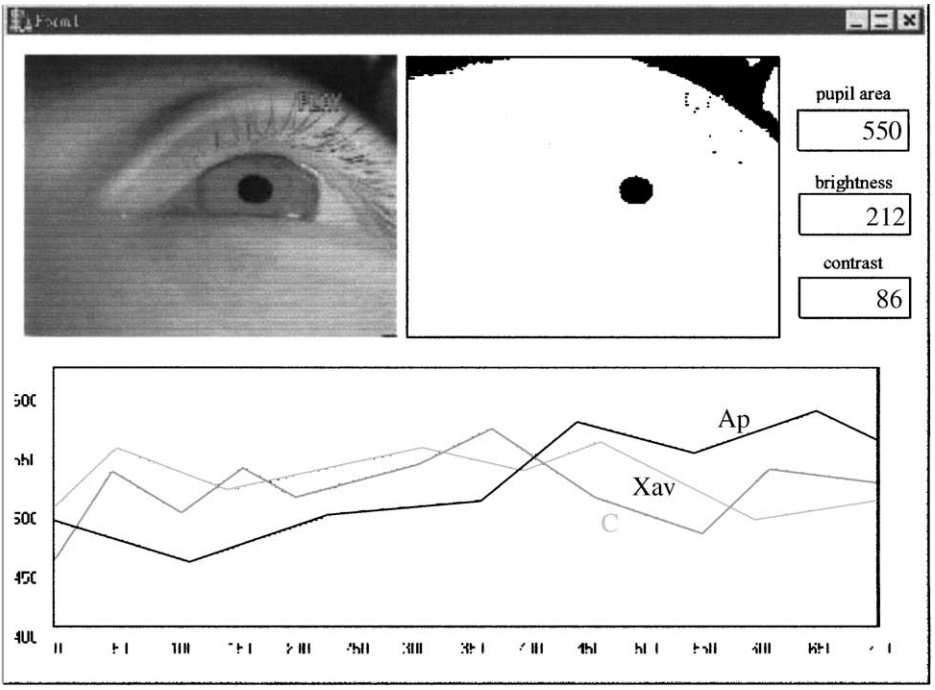

Fig. 6. A pupil-area measurement frame and statistical results for analyzing the brightness, contrast value of the image on the VR display device.

An NTSC video information signal is transmitted to the DSP unit. Fig. 7 shows how this analog signal represents the image brightness in this measurement system. H is the period of a horizontal scan line. The lower part of the voltage signal denotes the bright part of the image while the higher part denotes the dark part of the image. The signal between two triggering pulses indicates a horizontal scanning line and from the signals in the y direction, the value of brightness in an image is obtained. Subsequently, filter triggering signals in the x direction, which are over a threshold value. The remaining signals are the scanned signals in an image. A summation of the brightness of all scanned signals $\sum_{i=1}^{n} X_i$ is then calculated. The summation of the brightness $\sum_{i=1}^{n} X_i$ divided by the number of pixels, n, in an image is an average brightness $X_{\text{av}} = \sum_{i=1}^{n} X_i/n$. Thereafter, the average brightness X_{av} is output to a computer.

After the voltage signal transmission to the DSP unit, an average frame brightness value is calculated. A check is then made to determine if the image signal is over the average brightness value. The summation of image signal which exceeds $X_{\max}$ is divided by half of the number of pixels so that the average higher brightness value $X_{\max}$ is obtained. Accordingly, the average lower brightness value $X_{\min}$ can be obtained. So the contrast value C can be calculated by dividing $(X_{\max} - X_{\min})$ by $(X_{\max} + X_{\min})$. The contrast value is then output to a computer.

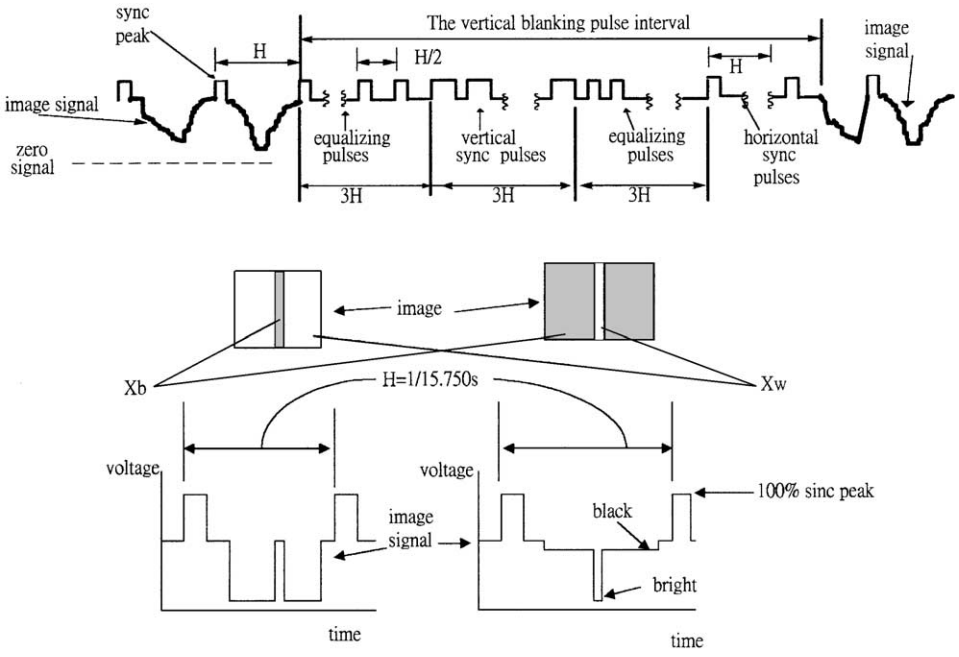

Fig. 7. The DSP unit calculates the average brightness and contrast value of images in the measurement system.

The position of camera (below the line of sight) causes significant distortion of the pupil, particularly when large eye movements are involved. Fig. 8 indicates that the eye movement relationships with the gazing directions are unique if the subject is gazing at different locations in a plane. Fig. 9(A) shows the calibration board for the eye-tracking device. On this board, the icons from "1" to "13" are used for the horizontal calibration, and the icons from "14" to "25" are used for the vertical calibration. Fig. 9(B) and (C) show examples of gazing data when a subject gazes at the horizontal and vertical lines. According to this database, the nonlinear mapping relationship between the center of the pupil image and the gaze location at the screen can be obtained. The subject gazes at targets "A", "B", "C", "D" to define the search range and the specified pupil size. When the utmost locations of the eye windows are determined, this region can be locked for advanced analysis (Fig. 10). This calibration process can also decrease the errors in the computation of both pupil diameter and its center spatial coordinates.

Five factors are used to evaluate the test conditions and eye movements: K_1, K_2, U_1, and U_2

2.1. The coefficient k_1 for the control ability of user

Here five points in the calibration process were adopted. After a standard configuration, the reference locations (P0, Q0), (P1, Q1), (P2, Q2), (P3, Q3), (P4, Q4) can be obtained for the center of the eye corresponding to the gazing icons 14, 13, 7, 1, 25 in Fig. 9(A). In Fig. 11, the geometric relationship of the five calibration points is shown.

The coefficient K_1 for the ability of the subject to control his gaze is defined as follows:

$$K_1 = \frac{\overline{L_{02}}\,\overline{L_{12}}\,\overline{L_{32}}\,\overline{L_{42}}}{\overline{L'_{02}}\,\overline{L'_{12}}\,\overline{L'_{32}}\,\overline{L'_{42}}},$$

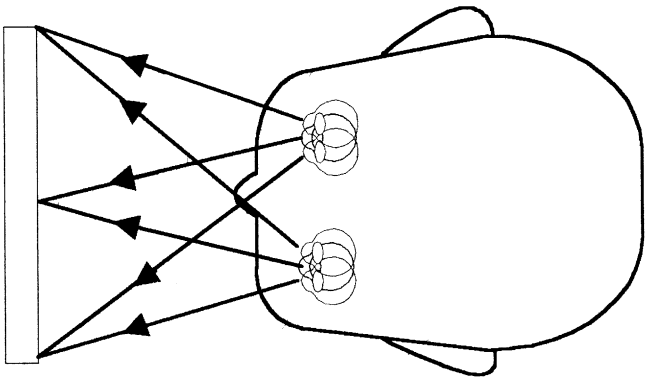

Fig. 8. The eye movements when the subject is gazing at different locations.

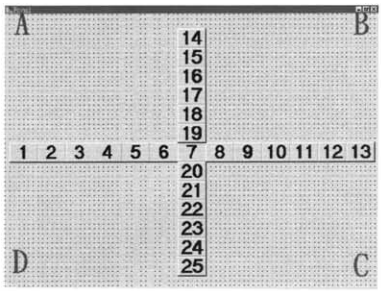

(A)

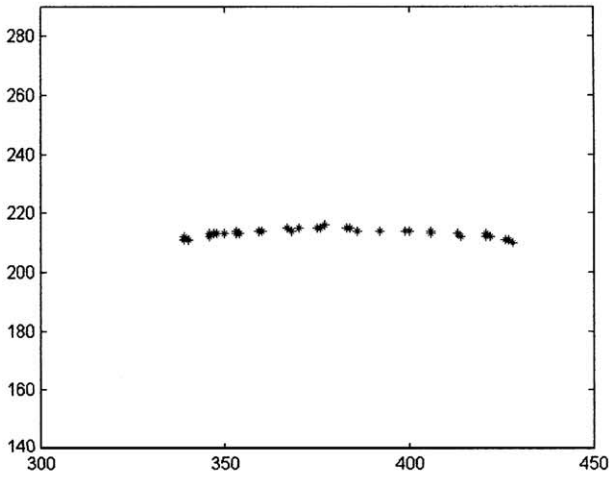

(B)

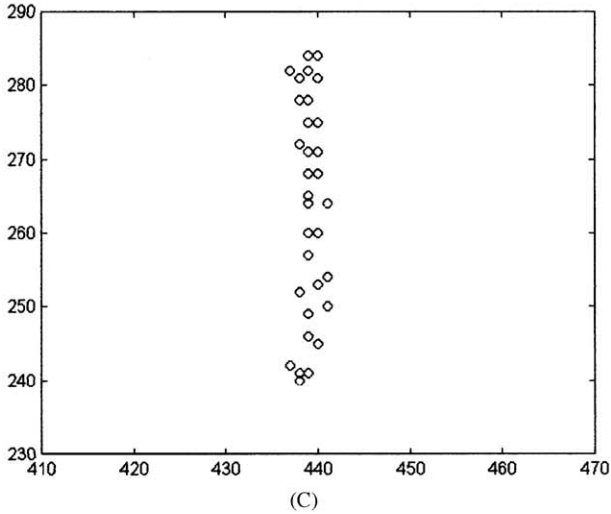

(C)

Fig. 9. (A) A calibration board for the eye-tracking device, (B) the data when the subject gazes at the horizontal line (unit: pixel), and (C) the data when the subject gazes at the vertical line (unit: pixel).

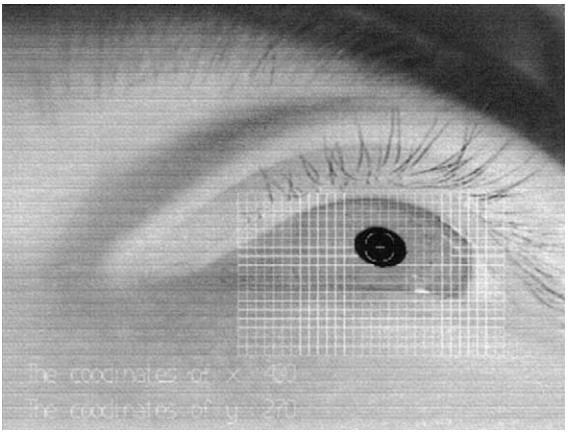

Fig. 10. Search range.

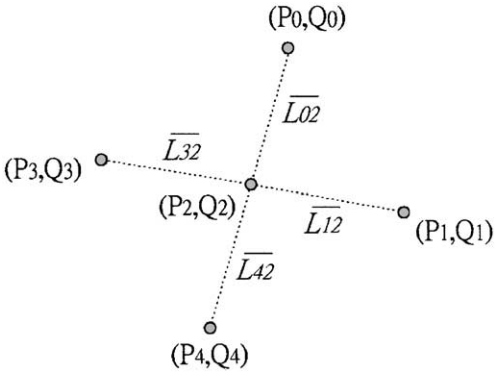

Fig. 11. The geometric relationship between the five calibration points.

Table 1
The ideal value for $\overline{L'_{02}}$, $\overline{L'_{12}}$, $\overline{L'_{32}}$, $\overline{L'_{42}}$ (unit: pixel)

$\overline{L'_{02}}$	$\overline{L'_{12}}$	$\overline{L'_{32}}$	$\overline{L'_{42}}$
33	55	55	37

where $\overline{L_{02}}$, $\overline{L_{12}}$, $\overline{L_{32}}$, and $\overline{L_{42}}$ are the distances between the center of the eye corresponding to the gazing icons. $\overline{L'_{02}}$, $\overline{L'_{12}}$, $\overline{L'_{32}}$, and $\overline{L'_{42}}$ are the ideal values, as indicated in Table 1. The ideal values were obtained using skillful eye-tracking device operators. In an ideal case $K_1 \approx 1$. A subject who has a unilateral horizontal gaze handicap (inability to gaze at a target on the right or left half of the screen) or unilateral vertical gaze handicap, will obtain a smaller K_1 value.

2.2. The coefficient K_2 for the gazing ability of user

The coefficient K_2 for the subject's gaze control ability is defined as follows:

$$K_2 = \frac{\overline{S_0}'}{\overline{S_0}} \frac{\overline{S_1'}}{\overline{S_1}} \frac{\overline{S_2'}}{\overline{S_2}} \frac{\overline{S_3'}}{\overline{S_3}} \frac{\overline{S_4'}}{\overline{S_4}},$$

where $\overline{S_0}$, $\overline{S_1}$, $\overline{S_2}$, $\overline{S_3}$, and $\overline{S_4}$ are the standard deviations of the center of the eye when the subject gazes at one point for a specified period. $\overline{S_0'}$, $\overline{S_1'}$, $\overline{S_2'}$, $\overline{S_3'}$, and $\overline{S_4'}$ are the ideal values, as indicated in Table 2.

When $K_2 \ll 1$, the subject may be inattentive or has poor gaze control ability at the fixed points.

2.3. The coefficient U_1 for the user's eye activity

After the calibration process, if the coefficients K_1 and K_2 for the subject are large enough to verify his ability for using this measurement system, the subject will be required to gaze at a rotating or random motion target on the screen for further testing. When the subject is gazing at the rotating target (Fig. 12(A)), the coefficient U_1 is used for the subject's eye activity and defined as follows:

$$U_1 = \frac{\sum_{n=1}^{N} A_n}{\pi N} = \frac{\bar{A}}{\pi},$$

where A_n is the angle between the eye's various tracks when the subject watches the rotating target, as shown in Fig. 12(B)

$$\begin{aligned}
A_{n-1} &= \angle P_{n-2}P_{n-1}P_n,\\
A_n &= \angle P_{n-1}P_nP_{n+1},\\
A_{n+1} &= \angle P_nP_{n=1}P_{n+2},\\
&\vdots\\
A_n &= \cos^{-1}\left(\frac{1}{2}\frac{\overrightarrow{P_nP_{n-1}} \cdot \overrightarrow{P_nP_{n+1}}}{\overline{P_nP_{n-1}}\ \overline{P_nP_{n+1}}}\right),\\
N &= m-2.
\end{aligned}$$

where m is the number of rotating points, $\bar{A}$ is the average angle between the various eye track.

When U_1 is close to 1, it means that the subject's eye activity is good. If U_1 is smaller than 0.2 when the rotation speed is slower than 0.15 round/s, it reveals that there may be some abnormality in the subject's neural system.

Table 2
The ideal value for $\overline{S_0'}$, $\overline{S_1'}$, $\overline{S_2'}$,$\overline{S_3'}$,$\overline{S_4'}$ (unit: pixel)

$\overline{S_0'}$	$\overline{S_1'}$	$\overline{S_2'}$	$\overline{S_3'}$	$\overline{S_4'}$
3	4	2	4	3

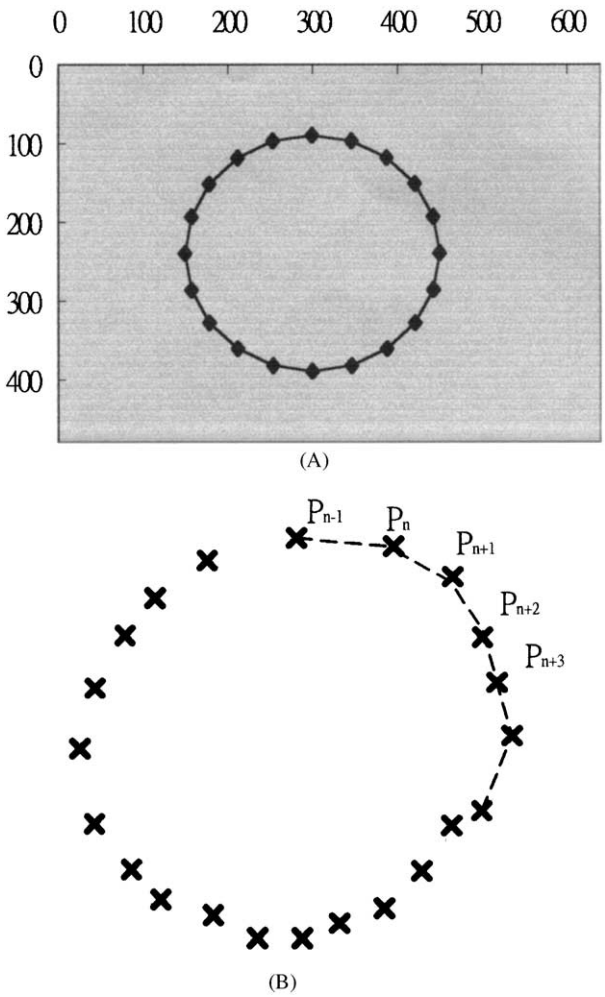

Fig. 12. (A) A rotating target at various speeds (unit: pixel), (B) the motions of center point of the eye when the subject is gazing at the rotating target, and (C) a random motion target (unit: pixel).

2.4. The coefficient U_2 for the user's concentration

When the subject is gazing at the rotating target, the coefficient U_2, is used for the subjects'concentration and is defined as follows:

$$U_2 = \frac{\sqrt{\sum_{n=1}^{N}(A_n - \bar{A})^2}}{\pi N}.$$

When $U_2 < 0.2$, it means that the subject has paid attention during this tracking test.

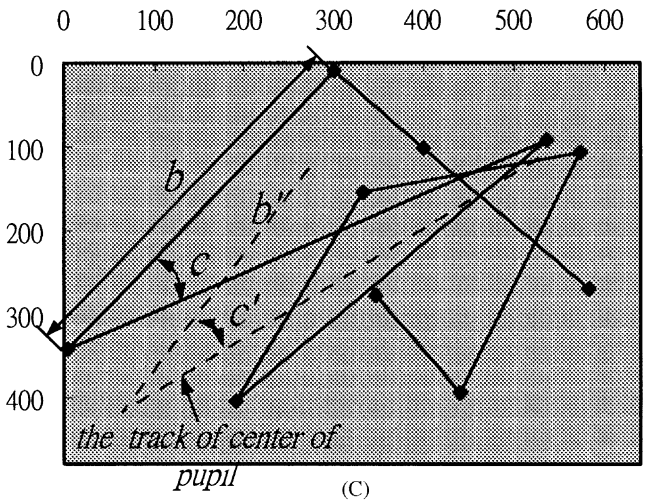

(C)

Fig. 12. (*Continued*).

2.5. The coefficient U_3 for the user's ability to move his eyes

When the subject is gazing at the random moving target, the coefficient U_3 indicates the subject's ability to move his eyes and is defined as follows:

$$U_3 = \frac{|(b - b')(c - c')|}{t_0 b' c'},$$

where b and c are the assumed length and angle between the center of the pupil when the subject is gazing at points in random motion, as shown in Fig. 12(C). Items b' and c' are the length and angle between the eye track when the subject watches a moving target. The time scale t_0 is the jump interval for a random motion target. The value U_3 reveals the degree of concentration by the subject and his ability to move his eye.

3. Hardware

The eye movement and VR display contrast and brightness data were recorded so that synthesized analysis concerning pupil dilation, contraction and eye movement could be completed. Comparing pupil contraction or dilation data with the image brightness/contrast of the VR, display device for helpful to research regarding the subjects' excitement.

This measurement system provides an apparatus for tracking eye movement and measuring pupil area. The apparatus is used by a subject viewing a VR display device and is comprised of:

1. a removable and attachable image capturing device (Fig. 13) for capturing an image of the subjects' eyeball in real time;
2. an image captures card, for receiving and processing the eyeball images, calculating the position of the center of the pupil and the entire pupil area;
3. a DSP unit for receiving and processing the video signals to obtain an average brightness value or an average contrast value;
4. a computer for receiving and analyzing the data from the image capture card and the DSP unit.

The (CCD) has a sensor with a low illumination intensity of 0.01 lx. This sensor can capture an image without an additional light source. In order to connect the CCD to computers or visors, an installation kit and various lenses are needed. One such installation kit is an angle adjustment element and the other is a mounting fixture element.

There are four types of VR systems: immersion VR, projection VR, desktop VR and simulator VR. The same hardware and software can be used for eye behavior measurement. The only additional component is the CCD lens for image formation at different distances. For example, the eye measuring system on the HMD uses a

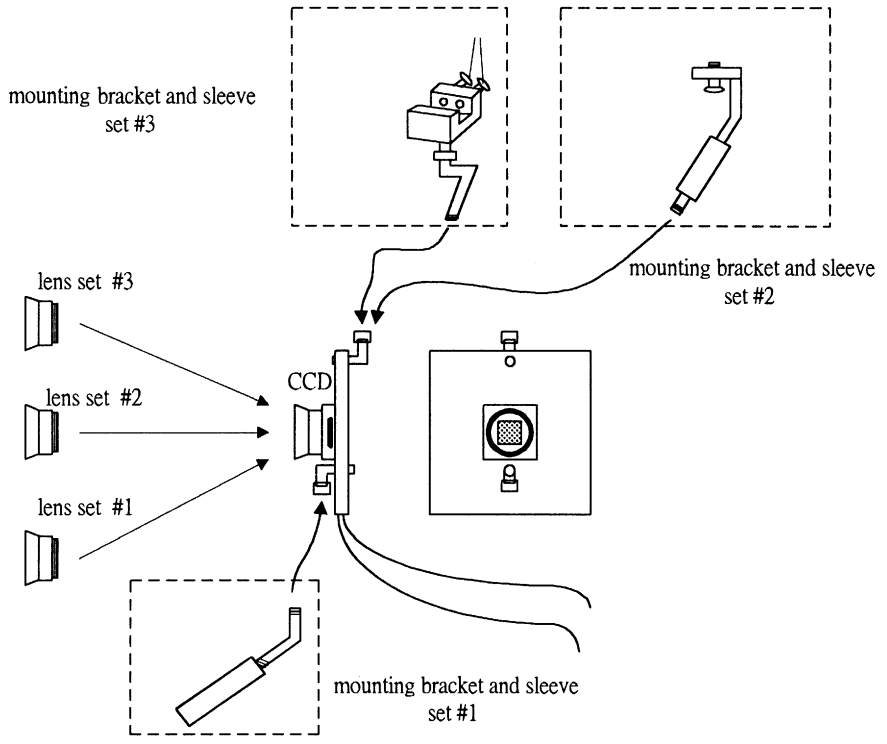

Fig. 13. CCD camera and the lens sets.

CCD that is placed very close to the eye. A special wide-angle lens is used in order to allow the eye to focus at such short distances. The effect of this device is image distortion, which makes straight lines appear curved. However, in the projection VR system (Fig. 14(A)), a lens with higher magnification is needed and the distortion problem is negligible. In Fig. 14(B), a CCD is mounted at the side of the monitor. In the simulator VR system, the player sits in a big simulator cabin and the CCD is mounted on the top of the cabin (Fig. 14(C)). Because it will be subjected to different geometrical and movement errors when the CCD camera is placed at various possible locations in VR systems, system calibration is needed.

The CCD lens can be adjusted to capture images. The lens set #1 is used in the installation kit for a heads-up VR display device for observing objects near the lens. Lens set #2 is used in a projection TV installation kit for observing objects far away from the lens. Lens set #3 is used in a personal computer installation kit and an installation kit for a platform-based simulator. In this measuring system, the

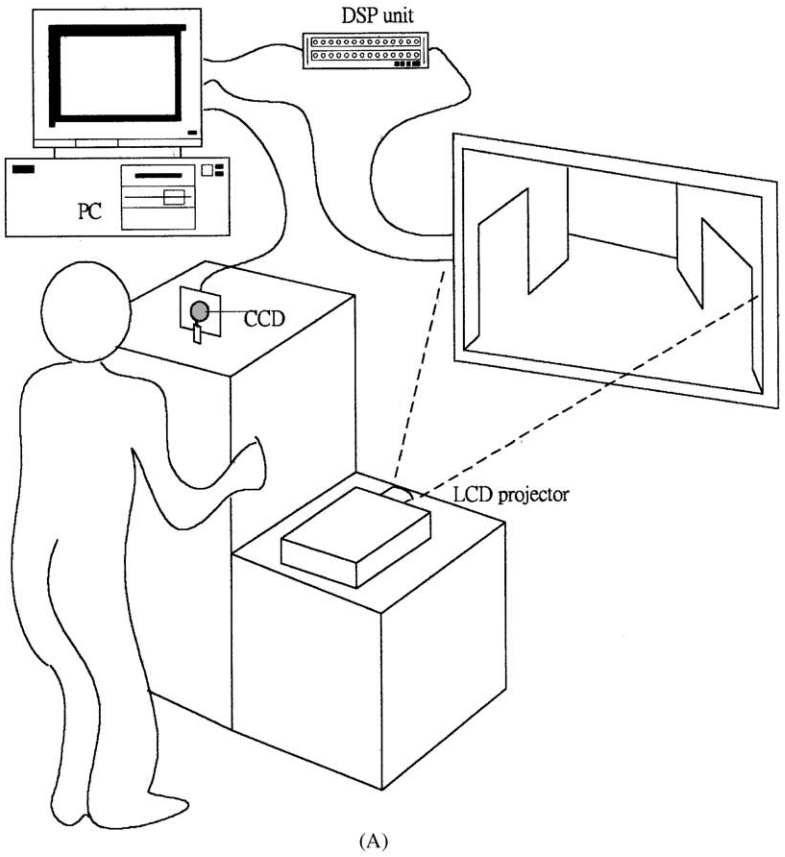

Fig. 14. (A) The eye measurement system setup for projection VR, (B) the eye measurement system setup for a desktop VR, and (C) the eye measurement system setup for simulator VR.

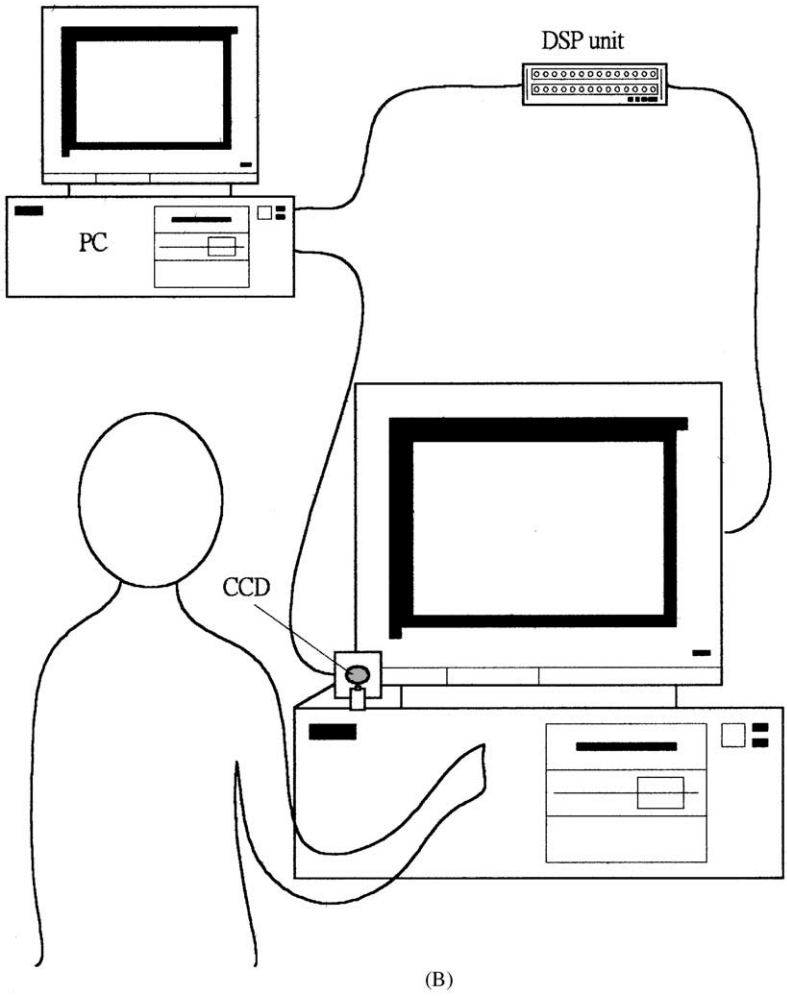

Fig. 14. (*Continued*).

installation kits can be used with one of the lenses mentioned above to obtain the desired observation result.

4. Experiments

In our experiments, data would typically be collected and analyzed on-line, i.e. we did not wait for the subject to complete the experimental task. The image analysis speed (about 12 frames/s on a Pentium III-500 computer), is a major characteristic of this system.

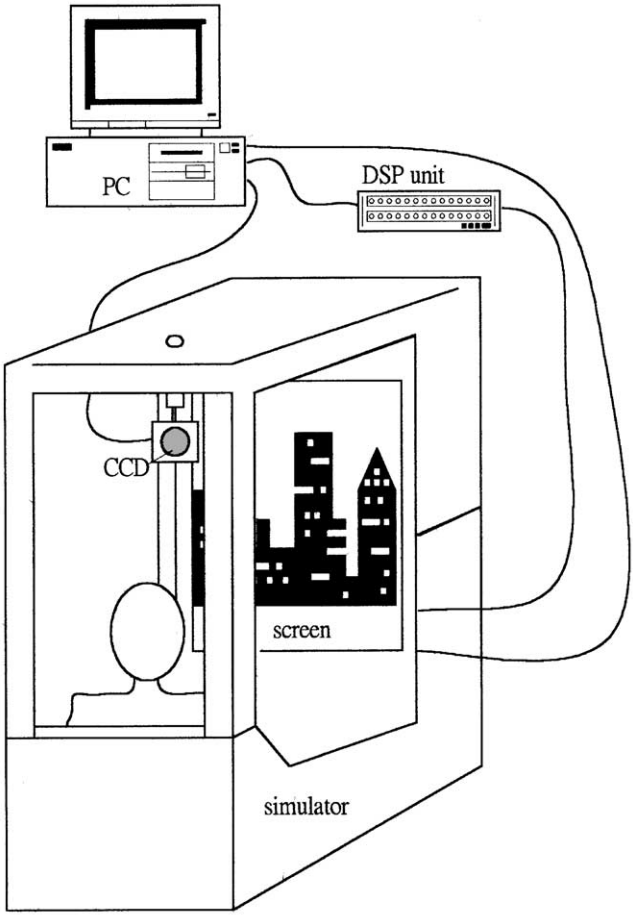

(C)

Fig. 14. (*Continued*).

We usually adopted the eye-tracking device with the head-mounted display system. This device configuration could make measurements regardless of how the user turned his head. The position of the center of the pupil provided an accurate representation of the eye's point of regard. A head orientation reference system was not necessary. This system can also communicate with a second computer, on which application programs can be performed. Calibrations were performed to compensate for system lags and errors, when presented with a rectangular board indicating different positions for eye gazing.

The curves in Fig. 15 represent the statistical results for the pupil area A_p, average brightness values X_{av}, and contrast values C, which can be illustrated in one chart or three charts. The coordinates can be slid by selecting "SLIDE". The window can be zoomed by selecting "ZOOM", and the zoomed window can be reversed by selecting

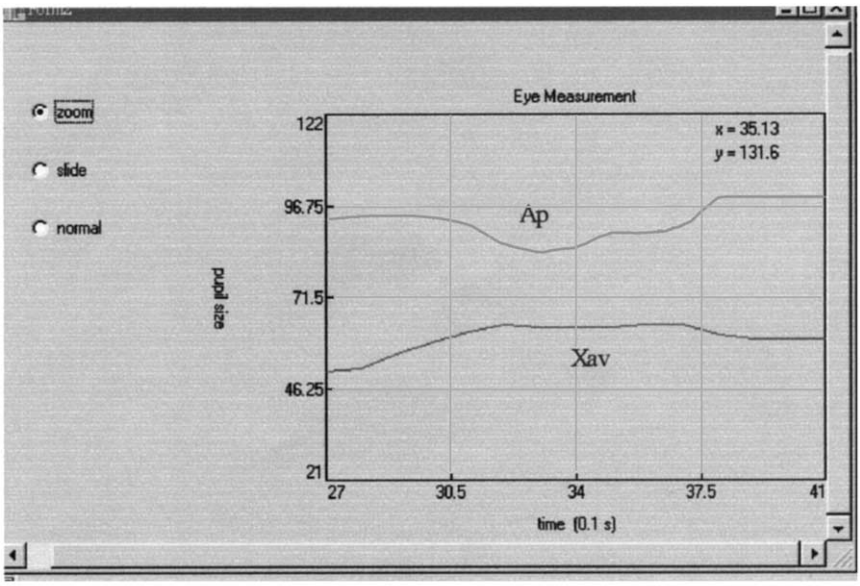

(A)

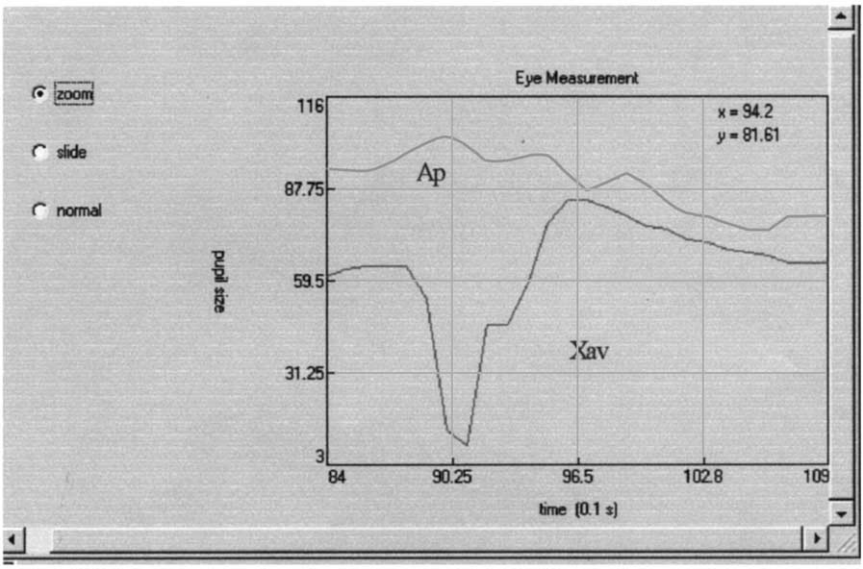

(B)

Fig. 15. The statistical pupil areas and average brightness values for images in the measurement system: (A) case 1, (B) case 2, (C) case 3, and (D) case 4.

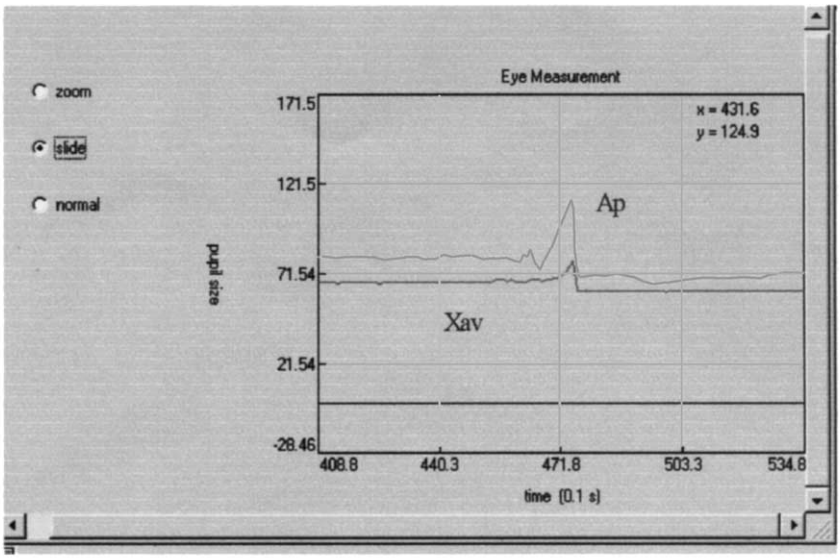

(C)

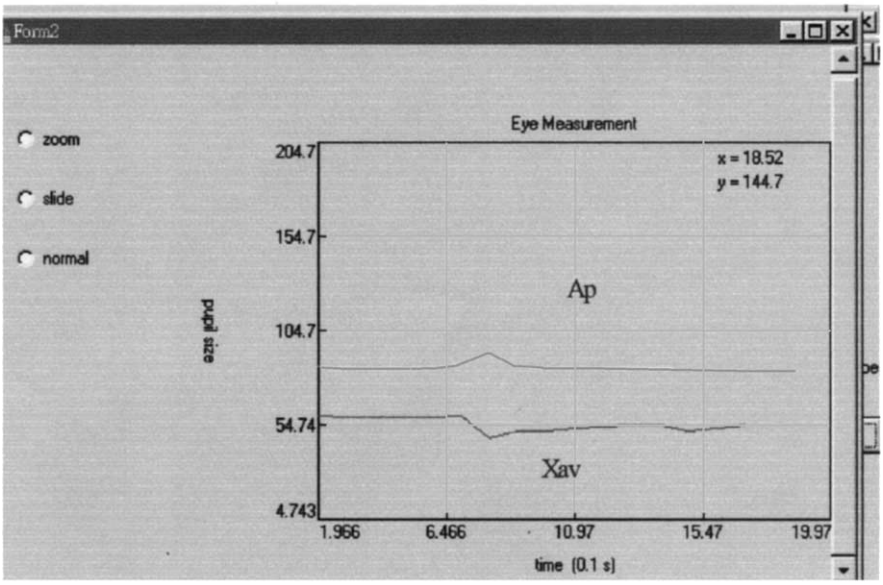

(D)

Fig. 15. (*Continued*).

"NORMAL" on the monitor screen. In Fig. 15(A), the upper curve represents the pupil area A_p statistical results. The lower curve represents the statistical result for the average brightness values X_{av}. The two curves show that the average brightness value X_{av} increased slightly followed by a slight decrease in the pupil area A_p.

When the user is watching the screen, the screen brightness and contrast will affect his pupil size. When the screen is bright, the pupil will shrink. When the contrast is low, the pupil will dilate. Here we neglect the contrast C and study the relation of the screen brightness, exciting degree of the user and his pupil size. In Fig. 15(B), the chart shows that if the curve representing the statistical average brightness value X_{av} fluctuates significantly (decreases in the beginning and then increases), the pupil area will increase slightly in the beginning and then decrease. In Fig. 15(C) chart, the pupil area A_p, evaluated in relation to the average brightness value X_{av}, the brightness value X_{av} increases suddenly and decreases subsequently, while at the same time the pupil area A_p also increases suddenly and decreases subsequently if the subject is watching an exciting movie. In normal, the value of the pupil area A_p will depend upon the average brightness value X_{av}. In this illustration, it can be seen that the effect of an exciting video is more important for the pupil area A_p than the average brightness value X_{av}. Scholars can use these data for psychometry studies.

Fig. 15(D) indicates that the average brightness value X_{av} decreases slightly in the beginning and then increases. The pupil area A_p increases slightly in the beginning and decreases subsequently indicating that the user is not interested and may not watch the screen. VR designers can therefore determine if the images on the VR display screen are attractive to people by reading these charts.

The human eye is much less sensitive to the details in moving images than in still images. The analysis data show that at high spatial frequency, the eye's sensitivity to temporal frequency decreases and similarly at high temporal frequency, the sensitivity to spatial frequency is diminished. By some simple aspect of visual acuity test, a doctor can judge if a patient has strabismus or nystagmus. However, if an object is moving with a velocity vector that is either constant or slowly changing, a viewer can then track the object by watching the subjects' eyes. This results in an

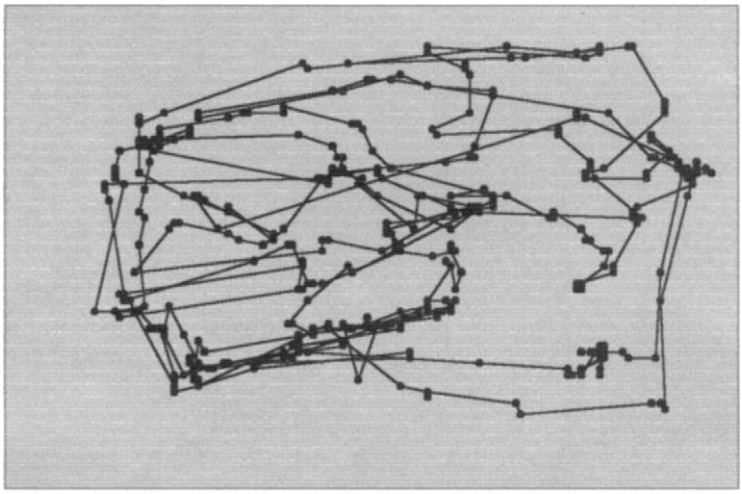

Fig. 16. The statistical locations of an eyeball track in the measurement system (unit: pixel).

image on the retina that has a constant view of the moving object while the background moves. Using this method, a doctor or other researchers could observe the patient's visual acuity ability more conveniently.

Fig. 16 represents pupil positions. Fig. 17 shows the result from connecting dotted marks, wherein the result shows the pupil movement priority. This program can be applied to measure the length of time that the pupil spends at a certain location. Fig. 18 shows a chart of the statistical location density for a

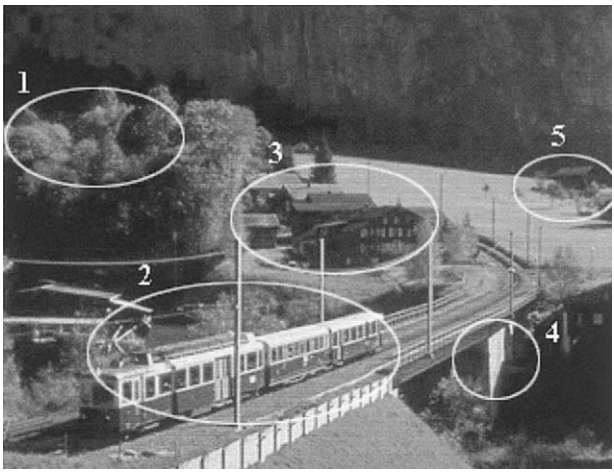

Fig. 17. The browsing priority in the image.

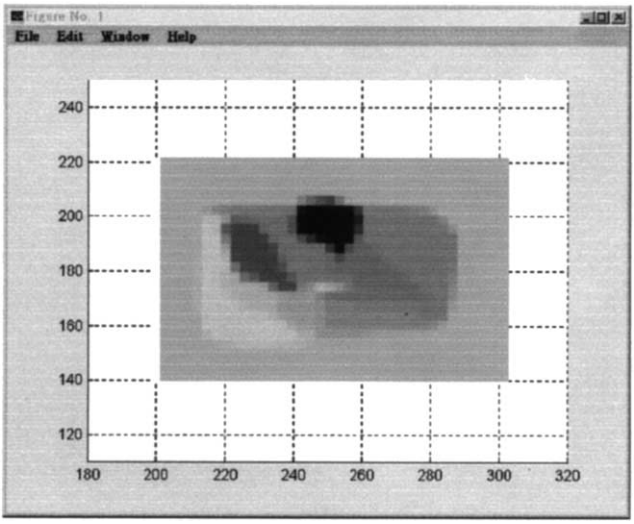

Fig. 18. The statistical gazing values are represented by the image density (unit: pixel).

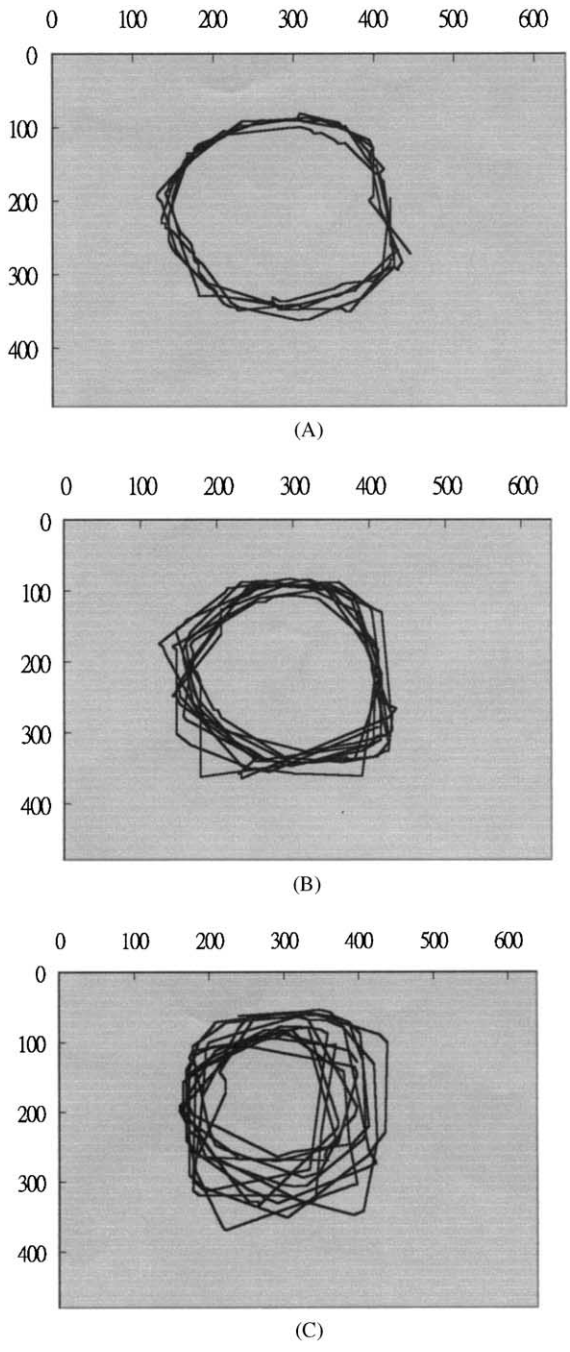

Fig. 19. The tracks for center point of the eye when the subject is gazing at the rotating target. The rotation speed is (A) 4 round/s, (B) 2 round/s, and (C) 1 round/s (unit: pixel).

pupil centroid. The period of time that the pupil spends at a location is converted into a gray scale image, where increasing darkness indicates increasing time. The dotted marks in the chart allow researchers (for example, psychologists) to determine as to which part of the VR display device attracts the subjects' attention.

We can multiply K_1 and K_2 to evaluate the ability of the user to use this measuring system at the beginning of the eye behavior test. The validity of the calibration process depends on the geometric arrangement of the eye-tracking system and the eye movement. Usually, the multiplication of K_1 and K_2 is between 0.7 and 0.9. If the multiplication of K_1 and K_2 is <0.5, the calibration procedure is invalid or the subject does not have the ability to use the eye-tracking system.

The demonstration of the parameters designing the subject's alertness and ability to carry out certain eye-movement tasks is shown as follows. Fig. 19 shows the tracks for the center point of the eye when the subject is gazing at the entire target. In Fig. 19(A), the rotation speed is 4 round/s, the value of U_1 is 0.91, and the value U_2 is 0.12. In Fig. 19(B), the rotation speed is 2 round/s, the value of U_1 is 0.78, and the value U_2 is 0.13. In Fig. 19(C), the rotation speed is 1 round/s, the value of U_1 is 0.52, and the value U_2 is 0.15.

Fig. 20 shows the tracks for center point of the eye when the subject is gazing at the random motion target. In Fig. 20(A), the speed is at an interval 0.5 s and the value of U_2 is 0.0151. In Fig. 20(B), the speed is at an interval 0.3 s and the value of U_2 is 0.0142. In Fig. 20(C), the speed is at an interval 0.15 s and the value of U_2 is 0.0107. We can see that when the speed is fast, the under- shoot and over-shoot in this saccade test will appear distinctively.

5. Conclusion

In this paper, we presented a new method for tracking the eye and comparing the position of the pupil. An eye-tracking interface can determine the position of a subject's pupil and map this position into a point on the display screen. This apparatus, the eye movement and pupil area measurement device can be applied in a VR system. The eye movement, pupil dilation, contraction, and data regarding the brightness and contrast of the VR display device can be observed and recorded. From this data, synthesized analysis of pupil dilation and contraction and eye movement can be carried out. The data for pupil size and location can be plotted vs. the average brightness and contrast of a VR video image in real time and utilized for research in psychometry, ophthalmology, physiology, and the design of a VR system.

Comparison of computer results with the eye observation measurement data demonstrated very good agreement and greater detail. The availability of this multipurpose measurement system with five measuring factors will be reconfirmed in further research. I believe that researchers will benefit from both the theoretical and the applied aspects of our work.

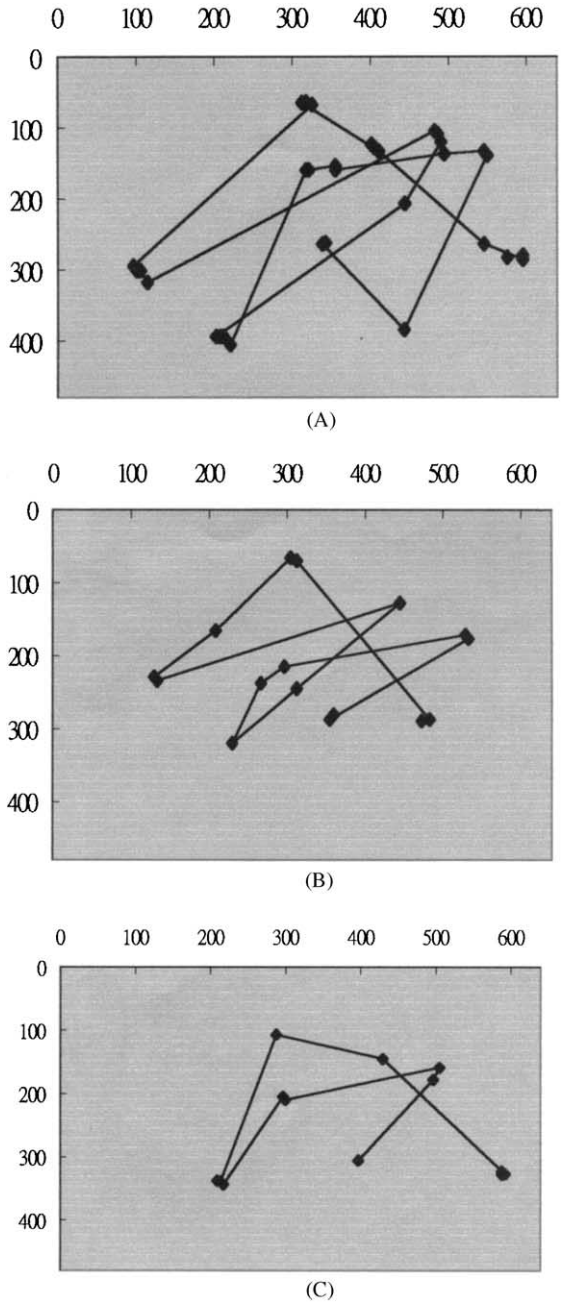

Fig. 20. The tracks of the center point of the eye when the subject is gazing at a random moving target. The speed was (A) 0.5 s/point, (B) 0.3 s/point, and (C) 0.15 s/point (unit: pixel).

Acknowledgements

This work is sponsored by the National Science Council, Taiwan, Republic of China under Grant No. NSC 88-2623-D-035-003.

References

[1] Burdea G, Coiffet P. Virtual reality technology. Wiley, New York, 1994, p. 47–79 [chapter 2].
[2] Pflibsen, et al. Eye fundus tracker/stabilizer. US Patent 4856891, 1987.
[3] Knapp, et al. Method and apparatus for eye tracking for convergence and strabismus measurement. US Patent 5293187, 1992.
[4] Gerhardt, et al. Eye tracking apparatus and method employing grayscale threshold value. US Patent 5481622, 1994.
[5] Grattan KT, Palmer AW. Interrupted reflection fiber optic communication device for the severely disabled. J Biomed Eng 1984;6:321–2.
[6] Grattan KT, Palmer AW, Sorrell SR. Communication by eye closure—a microcomputer-based system for the disabled. IEEE Trans Biomed Eng 1986;BME33:977–82.
[7] Liang CC, et al. System for monitoring eyes for detecting sleep behavior. US Patent 5570698, 1995.
[8] Kaufman AA, et al. Apparatus and method for eye tracking interface. US Patent 5360971, 1993.
[9] Chern-Sheng Lin. Methods for evaluating eye movements. ROC Patent 396032, 2000.
[10] Chern-Sheng Lin, Chih-Chung Chien, Yan-Jou Jan, Chin-Da Chen, Chiao-Hsiang Chen. Method and apparatus for tracking eye movement and measuring pupil area for application in a virtual reality system. ROC Patent 401291, 2000.
[11] Kirby M, Sirovich L. Applications of the Karhunen–Loeve procedure for the characterization of human faces. IEEE Trans Pattern Anal Mach Intell 1990;12(1):103–8.
[12] Canny J. A computational approach to edge detection. IEEE Trans Pattern Anal Mach Intell 1986;8(6):679–98.
[13] Brunelli R, Poggio T. Face recognition: features versus templates. IEEE Trans Pattern Anal Mach Intell 1993;15(10):1042–52.
[14] Chern-Sheng Lin, Chih-Chung Chien, Nanjou Lin, Chiao-Hsiang Chen. The method of diagonal-box checker search for measuring one's blink in eyeball tracking device. Opt Lasers Technol 1998;30(5):295–301.
[15] Xie X, Sudhaker R, Zhuang H. On improving eye feature extraction using deformable templates. Pattern Recognition 1994;27(6):791–9.
[16] White KP, Hutchinson TE, Carley JM. Spatially dynamic calibration of an eye-tracking system. IEEE Trans Systems Man Cybern 1993;23(4):1162–8.
[17] Amini AA, Weymouth TE, Anderson DJ. A parallel algorithm for determining two-dimensional object positions using incomplete information about their boundaries. Pattern Recognition 1989;22(1):21–8.